Available online at www.sciencedirect.com
ScienceDirect
Journal of Sound and Vibration 322 (2009) 740–755
JOURNAL OF SOUND AND VIBRATION
www.elsevier.com/locate/jsvi

Mode shape correction for wind-induced dynamic responses of tall buildings using time-domain computation and wind tunnel tests

K.M. Lam*, A. Li

Department of Civil Engineering, The University of Hong Kong, Pokfulam Road, Hong Kong

Received 15 May 2008; received in revised form 15 October 2008; accepted 29 November 2008
Handling Editor: J. Lam
Available online 20 January 2009

Abstract

The high-frequency force-balance (HFFB) technique is a common and effective wind tunnel testing method for the assessment of wind-induced dynamic responses of a tall building. The technique works in the frequency domain with the inherent assumption of ideal mode shapes so that the base moments can approximate the generalized forces. In this study, time histories of wind forces at several levels of a tall building model are obtained in the wind tunnel with a multi-channel pressure scanning system. This enables the building responses to be computed directly in the time domain for buildings with non-ideal mode shapes. Mode shape correction factors for the HFFB technique are thus obtained for the dynamic deflections and moments. The dependence of the mode shape correction factors on mode shapes and vertical distributions of wind excitation and building masses is investigated systematically. These correction factors are found to agree generally with the predictions proposed in previous studies but some differences are noted on the commonly assumed profiles of wind excitation and correction for torsion.

1. Introduction

Assessment of wind-induced dynamic responses is crucial in the design of a tall building. To date, wind tunnel testing remains the most reliable tool for this assessment and the high-frequency force-balance (HFFB) technique [1] has evolved to be the most versatile and widely used method. In this technique, a force balance is mounted at the base of a light and stiff model of the tall building to measure the fluctuating signals of base overturning moments and torsional moment on the entire building. The tall building is modeled as a multi-degree-of-freedom (mdof) system with concentrated masses and wind forces along the building height. Under the assumption of linear mode shapes in the sway directions (x, y) and constant mode shape in the torsional direction (φ), the base moments can approximate the generalized wind forces. Following the random vibration theory, the spectra of building deflections can be computed from the multiplication of the base moment

*Corresponding author. Fax: +852 2559 5337.
E-mail address: kmlam@hku.hk (K.M. Lam).

0022-460X/$ - see front matter © 2008 Elsevier Ltd. All rights reserved.
doi:10.1016/j.jsv.2008.11.049

spectra with the mechanical admittance function of the mdof model of the building. The computation is performed in the frequency domain and can adopt standard procedures in modal analysis [2].

The HFFB technique only accounts for wind-induced vibration of the first three fundamental modes, respectively, in the x, y and φ-directions and is based on the assumption of ideal mode shapes, that is linear sway modes and constant torsional mode. Although most tall buildings have sway mode shapes very near to linear, the torsional mode is also near to linear, rather than constant with height. An adjustment is commonly used by which a factor of 0.7 is applied to the φ-direction. A number of studies have investigated the effect of non-ideal mode shapes in a more rigorous manner [3–8]. Subsequently, recommendations are presently stated in quality assurance procedures on wind tunnel testing [9] that when the actual building mode shapes deviate significantly from the linear modes by more than 10%, corrections to the dynamic response from the base-balance technique are necessary.

Most of the reported investigations on mode shape correction factors are based on analytical studies. Nonlinear mode shapes of different power law variations with height are used in the analysis in which the wind-induced responses are computed and compared to those for ideal mode shapes. The wind-induced deflections also depend on the vertical distribution of wind forces as well as their correlation along the building height. With these distributions described by power law variation, mode shape correction factors are calculated as functions of the power law exponents for the mode shapes and the force distribution [4–6]. Holmes [4] and Xu and Kwok [5] consider the two limiting cases of high correlation and low correlation of wind excitation along building height and come up with different expressions of mode shape correction factors. In addition to mode shape correction factors for displacement, Boggs and Peterka [6] extend mode shape correction factors to the wind-induced dynamic moments with the inclusion of the additional effect of mass distribution along the building height.

A few wind tunnel measurements of wind-induced responses of tall building models of different mode shapes have been reported [7,8]. These limited experimental data are used in the analytical studies [4–6] for the comparison and validation of the proposed mode shape correction factors. However, the data only provide a few single cases of mode shapes and wind force distributions. This paper aims at a parametric investigation on the effect of non-ideal mode shapes on the HFFB evaluation of wind-induced deflections and moments of a tall building. The variables of mode shapes and vertical distributions of wind forces and masses are systematically changed in the investigation. Wind pressure on a tall building model is measured in a near-simultaneous manner with a multi-channel pressure scanning system. Time histories of wind forces and torsion on different levels of the building are obtained from pressure integration. Wind-induced deflections and moments of a tall building with non-ideal mode shapes are computed in the time domain by modal analysis.

With the advancement of high-speed multi-port pressure scanning instrumentation, time-domain computation of building responses is becoming more practical in wind tunnel testing [10]. By synthesizing time histories of wind forces at different building levels from pressure measurement, the technique also enables the assessment of coupled lateral and torsional modes of vibration of tall buildings [11] and the effect of eccentricities between the structural mass centre and the elastic centre [12]. The effect of coupled vibration modes on the assessment of wind-induced responses of a tall building with the basic HFFB technique can also be investigated by the time-domain technique. This can provide validation for the enhanced version of the HFFB technique to cater for complex mode shapes [13].

2. Mode shape correction factors from literature

The mode shape correction factors proposed in Refs. [5,6] are used for comparison with the results of this paper. Both studies were based on simplified analytical treatments in which the vibration mode shapes, ϕ, of the tall building are described by power law variation with height, z, as

$$\phi(z) = \alpha\left(\frac{z}{H}\right)^{\beta} \tag{1}$$

where H is the height of the building and α is the amplitude of mode shape at the top of the building. For many full-scale tall buildings, the power exponent β has values near 1.0 for both sway and torsional modes. The HFFB technique assumes $\beta = 1$ for the sway mode and $\beta = 0$ for the torsional mode. Boggs and Peterka [6]

used the power law to describe the variation of fluctuating wind excitation of shear forces and torsional moments, p, along building height as

$$p(z,t) = \alpha_P \left(\frac{z}{H}\right)^{\gamma} \cdot \psi(t) \tag{2}$$

where $\psi(t)$ is a fluctuating function of time. The power exponent γ describes the vertical distribution of wind excitations. No distinction was made between wind-induced vibration along the two sway directions and the mode shape correction factor for displacements in either sway direction was derived as

$$\eta_1 = \frac{\gamma+2}{\beta+\gamma+1} \tag{3a}$$

For torsional displacement, the mode shape correction factor was

$$\eta_{1z} = \frac{\gamma+1}{\beta+\gamma+1} \tag{3b}$$

In Xu and Kwok [5], the power law was used to describe the mean wind speed profile $\overline{U}(z)$ and the vertical distributions of wind forces were assumed proportional to $\overline{U}$ or $\overline{U}^2$, respectively, for along-wind or cross-wind and torsional excitations. Mode shape correction factors were derived for the two limiting cases of high correlation and low correlation of wind excitation along the building height. The correction factors were functions of the mode shape power exponent β and the power law exponent of the mean wind speed profiles and there were different expressions for the along-wind and cross-wind sway directions. However, when the power law exponents for the load excitations, γ, are used instead, the same expression is obtained for the mode shape correction factors in the two sway directions and the mode shape correction factors for the high-correlation case are identical to those in Eq. (3) from Ref. [6]. In other words, using the power law exponent of the wind force distribution makes it unnecessary to distinguish between along-wind and cross-wind responses and full correlation of wind excitation along the building height is implicitly assumed in Ref. [6]. For the low-correlation case of Ref. [5], the mode shape correction factors are re-written in terms of γ as

$$\eta_{1,\mathrm{low}} = \left(\frac{2\gamma+3}{2\beta+2\gamma+1}\right)^{1/2} \tag{4a}$$

$$\eta_{1z,\mathrm{low}} = \left(\frac{2\gamma+1}{2\beta+2\gamma+1}\right)^{1/2} \tag{4b}$$

In Boggs and Peterka [6], mode shape correction was extended to wind-induced dynamic moments and equivalent static forces. The proposed correction factors depended on the additional effect of mass distribution along the building height, $m(z)$. Linear variations were considered via a mass reduction factor λ:

$$m(z) = m_0 - (m_H - m_0)\left(\frac{z}{H}\right) == m_0\left(1 - \lambda \cdot \frac{z}{H}\right) \tag{5}$$

where m_0 and m_H are the masses at the base and top floor of the building. The proposed correction factors for base moments were

$$\eta_M = \frac{\gamma+2}{\beta+\gamma+1}\left(\frac{\beta+3-\lambda(\beta+2)}{2\beta+2-\lambda(2\beta+1)}\right)\frac{2(\beta+1)(2\beta+1)}{(\beta+2)(\beta+3)} \tag{6a}$$

The correction factor for torsional moments was

$$\eta_{Mz} = \frac{\gamma+1}{\beta+\gamma+1}\left(\frac{\beta+2-\lambda(\beta+1)}{2\beta+2-\lambda(2\beta+1)}\right)\frac{2(2\beta+1)}{\beta+2} \tag{6b}$$

3. Test building and wind tunnel tests

A square building was chosen as the typical tall building subjected to wind-induced responses. Measurements at a target geometric scale of 1:300 were made in the boundary layer wind tunnel of the

Department of Civil Engineering at the University of Hong Kong. It had a 3.0 m wide and 1.8 m tall working section in which wind characteristics of the open land terrain type were simulated in the test section with the installation of triangular spires and 8 m long fetch of floor roughness elements. The mean wind speed profile followed the power law with exponent 0.15. The turbulence intensity varied from a value of about 0.20 near ground to about 0.08 near the roof height of the model with a profile near to the power law with exponent −0.30. The building model was 50 cm tall with a square planform of size 10 cm × 10 cm. At a scale of 1:300, it represented a 53-storey prototype residential tall building 150 m tall and 30 m wide. The details of the wind tunnel characteristics and the choice of this tall building geometry have been described previously [14,15].

Fluctuating wind loads on the building were measured with the multi-channel pressure scanning technique. Pressure taps were installed at seven levels along the height of the building model at which surface pressure was measured simultaneously by five 32-port electronic pressure scanners (PSI, Inc.) mounted inside the model. On each level, there were 20 pressure taps, five on each of the four building faces. The sampling rate for each pressure tap was 100 Hz and the record length was 60 s. Time histories of wind forces along the two body axes, F_x, F_y and wind torsion, M_z, at each level were obtained from integration of the pressure signals with their associated tributary areas. These wind excitation forces could be converted into full-scale values corresponding to any prototype wind speed. In addition, a base-balance building model was also built and fluctuating base moments on the model were measured directly with a HFFB (JR3, Inc.).

The dynamic properties of the prototype test building were borrowed from a real 53-storey reinforced concrete residential building of similar size and shape. The first three vibration mode shapes $\phi(z)$ and the corresponding natural frequencies n_0 of that building had been determined by the finite element model ETABS. Fig. 1 shows the first three vibration modes. Due to symmetry of the building, the first two vibration modes, which were along the two sway directions, were almost identical and with almost the same natural frequencies. There was almost zero mode coupling from other directions. The third vibration mode was along the torsional direction φ with some mode coupling. The distribution of building masses along the building height affected the dynamic moments [6] and for the real residential building, the building masses are uniform from the third storey onwards. The lower floors were podium levels and had heavy masses.

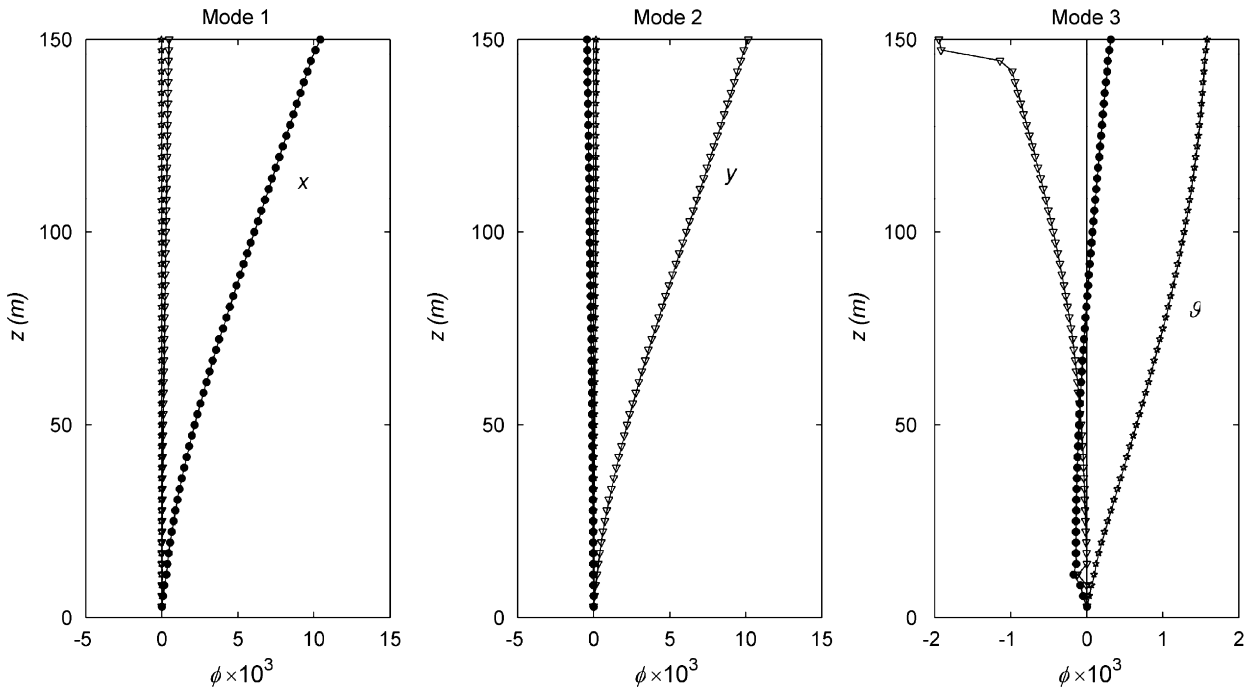

Fig. 1. Vibration mode shapes of full-scale test building. Natural frequencies: mode 1: 0.234 Hz; mode 2: 0.247 Hz and mode 3: 0.415 Hz.

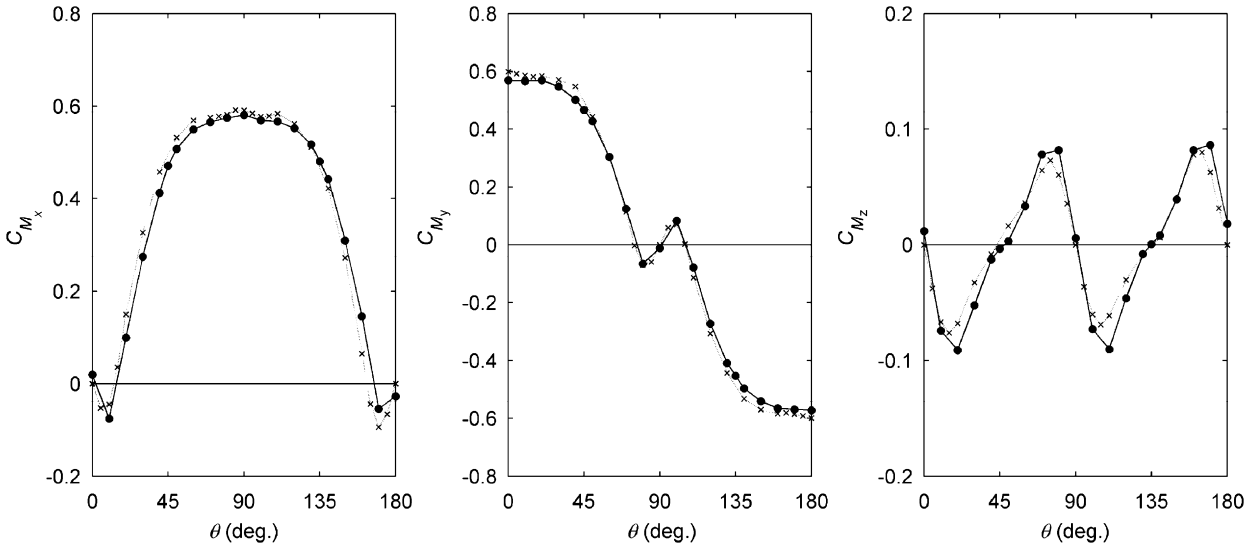

Fig. 2. Mean moment coefficients. ●: from pressure integration and ×: direct base balance measurement.

Measurements were carried out at a number of wind incidence angles θ to the square building. Fig. 2 shows the variation of mean moment coefficients on the entire building with wind angles. The building height H, building breadth B and the unobstructed mean wind speed $\overline{U}_H$ at height H are used to calculate the force and moment coefficients of C_{F_x}, C_{F_y}, C_{M_x}, C_{M_y} and C_{M_z} using equation such as

$$C_{F_x} = \frac{F_x}{1/2(\rho \overline{U}_H^2 BH)}$$

$$C_{M_x} = \frac{M_x}{1/2(\rho \overline{U}_H^2 BH^2)}$$

$$C_{M_z} = \frac{M_z}{1/2(\rho \overline{U}_H^2 B^2 H)} \tag{7}$$

Force and moment coefficients are used for mean and fluctuating loads on the entire building as well as the loads on different sections of the building. Fig. 2 shows that the moments on the entire building model obtained from pressure integration agree very well with those from direct HFFB measurement.

4. Characteristics of wind forces

Histories of wind forces on the seven levels of the building model are obtained from integration of pressure signals and the vertical distributions of mean and root-mean square (rms) force and torsion coefficients at some representative wind angles are shown in Fig. 3. While mean wind loads generally increase with height, rms values of the fluctuating loads are found to decrease with height. This means that the power law exponent γ for the wind loads is negative instead of one or two times the positive exponent of the mean wind speed profile [5]. Furthermore, the experimental results in Fig. 3 suggest that the power law can be a crude approximation to the vertical distribution of wind excitation.

The cross correlation coefficients among wind force fluctuations on the seven levels are calculated and presented in Table 1. At wind angle $\theta = 0$ where F_x is the along-wind excitation, the correlation is rather low. The cross correlation coefficient between forces on the two highest levels is the largest but still only has value at about 0.5. At $\theta = 90^\circ$, F_x becomes the cross-wind excitation and much higher correlation exists along the

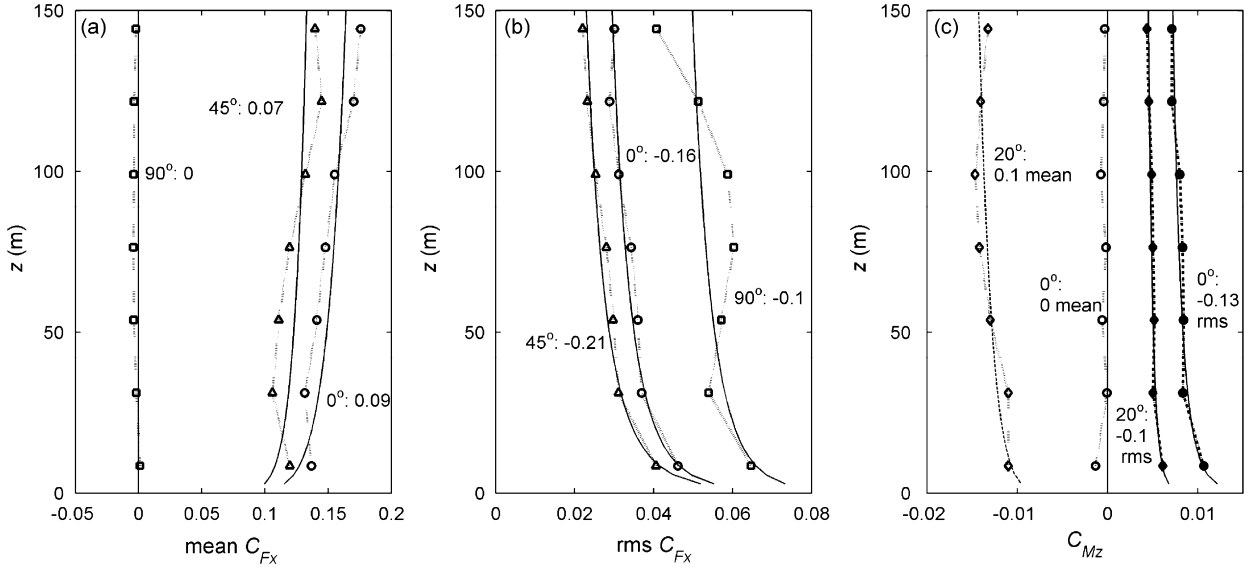

Fig. 3. Vertical distribution of wind excitation. Symbols: wind tunnel data and line: power law fit with exponent listed after wind angle.

building height. The cross correlation coefficients among adjacent levels have values between 0.8 and 0.5. At oblique wind angle such as $\theta = 45^{\circ}$ in Table 1, the correlations are lower than those at normal incidence. For the wind torsion, highest correlation occurs at normal incidence, $\theta = 0$ and the cross correlation coefficients between adjacent levels have the largest value at about 0.5. The results in Table 1 suggest that excitations in the along-wind and torsional directions are poorly correlated while there are some correlations in the cross-wind excitations.

5. Time-domain analysis of wind-induced responses

With the histories of wind forces available along the building height, wind-induced vibration of the building is computed in the time domain. Modal analysis is applied to simplify the computation. The 53-storey test building is modeled as a 53×3 dof system and its vibration in a particular vibration mode is represented by the generalized coordinate $q(t)$ and the equation of motion is

$$\mathbf{M} \cdot \ddot{q} + \mathbf{C} \cdot \dot{q} + \mathbf{K} \cdot q = P(t) = \phi^{\mathrm{T}} \cdot p(t) \tag{8}$$

where **M**, **C** and **K** are the generalized mass, damping and stiffness matrices, respectively. The generalized force vector P is obtained from the product of mode shape vector ϕ and force time history $p(t)$. The matrices **M**, **C** and **K** and the mode shape are available from the ETABS model of the building. Time histories of wind forces at all 53 storeys are obtained from those at the seven tapping levels by linear interpolation. In the HFFB technique with the assumption of ideal mode shapes, the right-hand side of Eq. (8) represents the base moments which are measured by the force balance. In this study, the pressure measurement enables $p(t)$ to be physically obtained and the generalized forces under non-ideal mode shapes can be computed.

Computation of Eq. (8) is carried out by direct time integration using the Newmark-β method [16]. Displacement responses are obtained from the combination of mode shapes and generalized coordinates over a sufficient number of modes:

$$x(z, t) = \phi(z) \cdot q(t) \tag{9}$$

Similar to the HFFB technique, structural damping is considered via a suitable value of damping ratio ζ. Histories of vibration-induced forces and torsion at every storey of the building are calculated from the building displacements and accelerations. Mean, rms values and power spectral density (psd) functions of all building responses and dynamic loads can be obtained from the time histories.

Table 1
Correlation coefficients between wind excitation on different levels of test building.

	Top-level	6	5	4	3	2	Bottom-level
F_x, $\theta = 0^\circ$							
Top-level	1						
6	0.52	1					
5	0.36	0.35	1				
4	0.41	0.30	0.22	1			
3	0.08	0.44	0.29	0.07	1		
2	0.23	−0.06	0.52	0.15	0.13	1	
Bottom-level	0.20	0.31	−0.27	0.51	0.10	−0.12	1
F_x, $\theta = 90^\circ$							
Top-level	1						
6	0.75	1					
5	0.67	0.79	1				
4	0.59	0.64	0.74	1			
3	0.37	0.49	0.61	0.67	1		
2	0.28	0.15	0.43	0.46	0.61	1	
Bottom-level	0.20	0.17	0.07	0.43	0.43	0.50	1
F_x, $\theta = 45^\circ$							
Top-level	1						
6	0.44	1					
5	0.34	0.24	1				
4	0.43	0.26	0.02	1			
3	−0.05	0.44	0.25	−0.18	1		
2	0.22	−0.19	0.59	0.07	−0.02	1	
Bottom-level	0.16	0.34	−0.41	0.63	0.06	−0.28	1
M_z, $\theta = 0^\circ$							
Top-level	1						
6	0.47	1					
5	0.33	0.48	1				
4	0.21	0.25	0.47	1			
3	0.08	0.13	0.23	0.49	1		
2	0.03	−0.05	0.09	0.20	0.42	1	
Bottom-level	0.00	−0.01	−0.09	0.11	0.23	0.32	1

As an example, Fig. 4 shows a part of the time histories of along-wind and cross-wind excitation moment at the base of the building, $C_{M_y}(t)$ and $C_{M_x}(t)$ and the along-wind and cross-wind deflections at the building top floor, $x(t)$ and $y(t)$, computed for the wind angle $\theta = 0$. The time-domain computation is carried out in full-scale assuming a wind speed at $\overline{U}_H = 52\,\mathrm{m/s}$ and a damping ratio at $\zeta = 0.02$. This wind speed is the 50-year return design value in the Hong Kong Wind Code 2004 [17] at 150 m height, representing typical strong wind conditions in typhoon-prone regions. The damping ratio at 2% is commonly used for responses under strong wind conditions. With Eq. (7), time histories of wind forces and wind torsion obtained at each level of the wind tunnel model are converted to their corresponding full-scale values at the chosen full-scale wind speed of 52 m/s. The time axis, t, also needs to be converted to full scale by the time scale λ_t which is determined by the length scale λ_L and velocity scale λ_U of the wind tunnel tests:

$$\lambda_t = \frac{t_{\text{model}}}{t_{\text{full-scale}}} = \frac{\lambda_L}{\lambda_U} = \frac{\lambda_L}{\left(\dfrac{\overline{U}_{H,\text{model}}}{\overline{U}_{H,\text{full-scale}}}\right)} \tag{10}$$

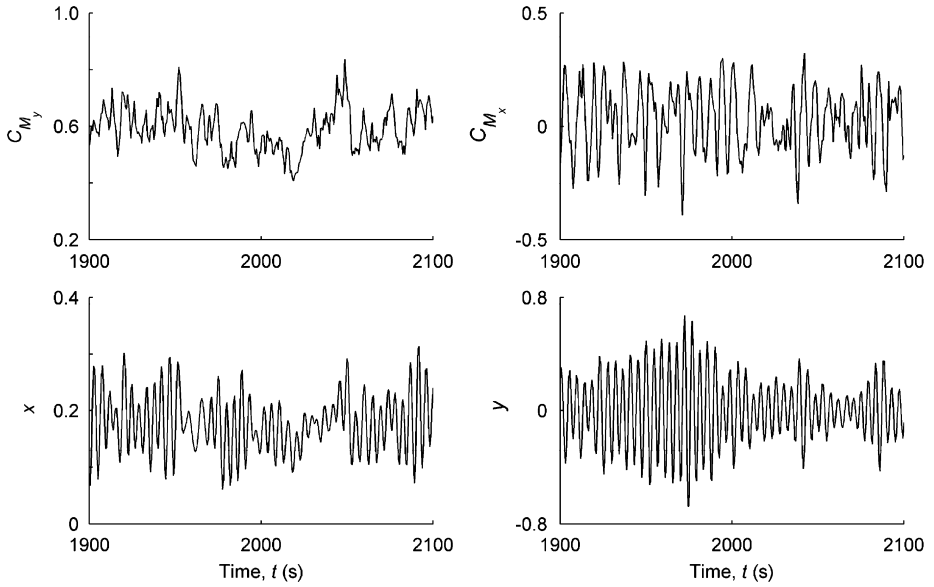

Fig. 4. Examples of time histories of base moments and top-floor deflections (in m) computed by time-domain technique. Wind incidence along x-direction ($\theta = 0$).

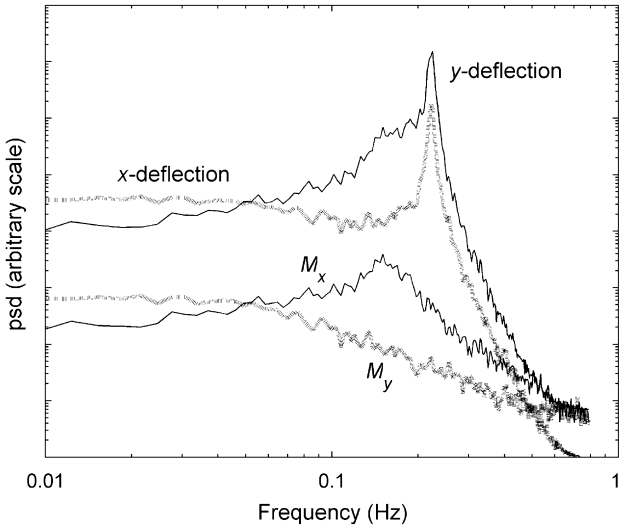

Fig. 5. Power spectra of wind excitation base moments and top-floor deflections from time-domain technique. Wind incidence along x-direction ($\theta = 0$).

The length scale in use is $\lambda_L = 1{:}300$ and the velocity scale is obtained from the ratio of $\overline{U}_H$ in the wind tunnel to 52 m/s.

The psd of the base moments and the computed dynamic deflections corresponding to the loading example in Fig. 4 are shown in Fig. 5. The moments are the excitation from the incidence turbulence wind actions as measured by a HFFB at the model base or obtained from integration of measured wind pressure. They do not include the dynamic magnification due to wind-induced building movements. Typical of a square tall building, fluctuations in the along-wind moment M_y are caused by turbulence buffeting without any dominant spectral components while fluctuations in the cross-wind moment M_x are characterized by vortex excitation. The cross-wind moment spectrum exhibits a sharp peak near $n = 0.15$ Hz and the corresponding Strouhal number at $nB/\overline{U}_H \approx 0.09$ is typical of vortex shedding from a square tall building. The natural frequency of building

vibration in either sway mode is around $n_0 \approx 0.24$ Hz and there is some mild resonant cross-wind response at this wind speed. The rms top-floor deflections are $\sigma_x = 0.057$ m and $\sigma_y = 0.180$ m. From the deflection histories of the building floors, wind-induced dynamic forces on each storey are computed as the inertial forces. The dynamic base moments are obtained subsequently. The rms overturning moments, which include the background excitation in Fig. 5 and the resonant response part, are $\sigma_{My} = 1.39 \times 10^8$ Nm and $\sigma_{Mx} = 6.11 \times 10^8$ Nm.

When the HFFB technique is used, ideal mode shapes are assumed and the excitation base moment spectra in Fig. 5 represent the psd of the generalized force $P(t)$ in Eq. (8). Computation is performed in the frequency domain from which the psd of the generalized coordinates q in Eq. (8) are solved. The deflection spectra are obtained through the frequency-domain counterpart of Eq. (9). In this step, only the mode shape values at the building top floor are used. In actual HFFB tests, base moments are measured directly by the base balance but in this study they are obtained from integration of wind pressure. The mean, rms values and psd of these moments have been checked to agree well with those from an actual HFFB measurement. Thus, it is possible to obtain the deflection responses of the test building as assessed by the HFFB technique. In the example of normal wind incidence at a wind speed of 52 m/s, the rms top-floor deflections from the HFFB technique are $\sigma_{x\text{-linear}} = 0.064$ m and $\sigma_{y\text{-linear}} = 0.202$ m. These values are obtained from the square roots of the areas under the deflection spectra.

The mode shape correction factors could be calculated from the ratio between the two sets of deflection values, such as

$$\eta_1 = \frac{\sigma_x}{\sigma_{x\text{-linear}}} \quad \text{and} \quad \eta_M = \frac{\sigma_{Mx}}{\sigma_{Mx\text{-linear}}} \tag{11}$$

For the example case, the correction factors are $\eta_1 = 0.887$ for the x-deflection and $\eta_1 = 0.888$ for the y-deflection. The mode shapes of these sway modes in Fig. 1 can be approximated by the power law of exponent $\beta = 1.36$. The wind force profiles in Fig. 3 are approximated by $\gamma = -0.16$ for F_x and $\gamma = -0.1$ for F_y. With these parameters, Eq. (3) gives $\eta_1 = 0.836$ for x and $\eta_1 = 0.841$ for y under the high-correlation case. The correction factors for the low-correlation case of Eq. (4) are $\eta_{1,\text{low}} = 0.888$ for x and $\eta_{1,\text{low}} = 0.892$ for y. It is evident that Eqs. (3) and (4) make good predictions to the presently obtained mode shape correction factors considering the different degrees of correlation for the along-wind (x) and cross-wind (y) excitation (Table 1).

6. Parametric study of mode shape correction factors

The wind tunnel measurements and ETABS model of the building in this study only provide a few cases of wind load characteristics and structural properties. In this section, the information is used to provide an extended set of wind loading cases through numerical adjustment so that a parametric study can be carried out.

To obtain all possible cases of wind loading characteristics in addition to those in Fig. 3, the vertical distribution of wind excitation is adjusted to any desired value of γ by multiplication of the wind load histories at each floor with an appropriate factor so as to satisfy Eq. (2). After this adjustment, characteristics of wind load fluctuations such as the spectral distribution in the force spectra remain unchanged. Most importantly, the correlation of wind forces along the building height is not affected by the adjustment.

On the dynamic properties of the building, it is desirable to cover all possible mode shapes. The mode shapes corresponding to different values of β following Eq. (1) can be readily produced artificially. However, with the adjustment of mode shapes, other structural properties need to be changed accordingly. In particular, it is necessary to adjust the building masses and the value of α so that the following requirement is still satisfied:

$$\phi^{\mathrm{T}} \cdot m \cdot \phi = \sum \left[m_0 \cdot \left(1 - \lambda \cdot \frac{z}{H}\right)\right] \cdot \left[\alpha \left(\frac{z}{H}\right)^{\beta}\right]^2 = \mathbf{I} \tag{12}$$

where $\mathbf{I}$ is the identity matrix. For the mode shape correction factors on wind moments and torsion, it is also possible to use a vertical distribution of building masses with any chosen value of mass reduction factor λ.

Wind-induced dynamic deflections and moments of the test building are computed in the time domain for a large number of loading cases with the test parameters systemically varied. The parameters include the power exponents β and γ, respectively, for the mode shapes and vertical profiles of wind excitation and the mass reduction factor λ. The corresponding response predictions using the HFFB method are computed as well, assuming ideal mode shapes. Thus, mode shape correction factors for deflections and moments are obtained for all loading cases. In this paper, results are presented mainly for the case of wind speed at $\overline{U}_H = 52\,\mathrm{m/s}$ and damping ratio at $\zeta = 0.02$. Investigations have been made at other wind speeds covering background response at low speeds to well beyond resonant response regime and damping ratios between 1% and 5%. The results show that the mode shape correction factors are not sensitive to these two parameters. Correction factors to the wind-induced building responses are mainly shown by the results at normal wind incidence ($\theta = 0$) at which the sway responses are in the along-wind and cross-wind directions and the torsion fluctuations are the largest (Fig. 3).

Fig. 6 shows the mode shape correction factors for deflections. Results are shown for four values of γ at $\gamma = -0.2$, 0, 0.2 and 0.4. Previous studies investigated positive values of γ only because it was usually believed that the vertical profile of wind excitation is proportional to the first or second power of the mean wind speed profile [6]. The wind tunnel measurements in this study show, instead, that negative values of γ can be commonly found, that is the rms values of wind excitation decrease with height. The present results, some not shown here, also suggest that the mode shape correction factors for γ greater than 0.4 do not differ much from those at $\gamma = 0.4$.

For the two sway directions, the dependence of η_1 on γ is more significant at lower values of γ. Furthermore, when γ becomes negative, even larger corrections are necessary for nonlinear mode shapes ($\beta \neq 1$). In most cases, the present data of η_1 lie between the curves of Eqs. (3a) and (4a). For the along-wind deflection, our correction factors are well predicted by Eq. (4a) for the low-correlation case. This is consistent with the actual correlation measurement of the along-wind excitation in Table 1. The table also shows that the correlation of cross-wind excitation is higher and this explains why the present data of η_1 for cross-wind deflections lie between the two prediction curves. It can be observed in Fig. 6 that the difference between the low-correlation and high-correlation prediction curves becomes less when γ becomes smaller and negative. For the variation with β, there are larger differences between the two curves when β departs from $\beta = 1$ to <1 than the other direction. Most real tall buildings have mode shapes with β near 1 and within the more usual range of β between 0.5 and 1.5, the mode shape correction factors have values within $\eta_1 = 1.0 \pm 0.2$. As expected, η_1 becomes less than 1 for $\beta > 1$.

For torsional responses, the ideal mode shape assumed in the HFFB technique is a constant mode shape, that is $\beta = 0$, where no correction is necessary, that is $\eta_{1z} = 1$. For practical values of $\beta > 0$, Fig. 6 shows that the correction factors for torsional deflections are always smaller than unity. As the mode shape deviates farther from the ideal case, more corrections are needed and the values of η_{1z} is more significantly different from unity when compared with η_1 for the sway responses. Similar to η_1, more severe correlation becomes necessary for negative values of γ. For the most extreme case of $\gamma = -0.2$ and $\beta = 2$ in Fig. 6, a correction factor as severe as $\eta_{1z} = 0.41$ is required. Low correlation is measured on the torsional excitation in Table 1 and the present data of η_{1z} lie very close to the low-correlation curve of Eq. (4b). When the HFFB technique is used, a correction factor at 0.7 is usually recommended for torsion [1]. It is observed from Fig. 6 that this value applies to the present data of η_{1z} for β near 1 and γ near 0.4.

As a first attempt to investigate the effect of building geometry, wind tunnel measurement is also made on a circular building model. The model has the same external dimensions as the square building model, that is a height at 50 cm and a diameter of planform at 10 cm. Pressure taps are installed on seven levels along its height and there are 18 pressure taps on each level. Due to the circular planform of the building, measurements are performed at one wind incidence angle only. Fig. 7 shows the distribution of mean and rms force coefficients along the height of the building. The mean along-wind force coefficient increases with height while the cross-wind force coefficient always has a mean value near zero. As expected for a circular building from which vortex shedding occurs, the rms cross-wind force coefficient is higher than the rms along-wind force coefficient. However, unlike the square building in Fig. 3, both rms force coefficients generally increase with height and the fitted power law exponent γ has a positive value for both coefficients. The cross correlation

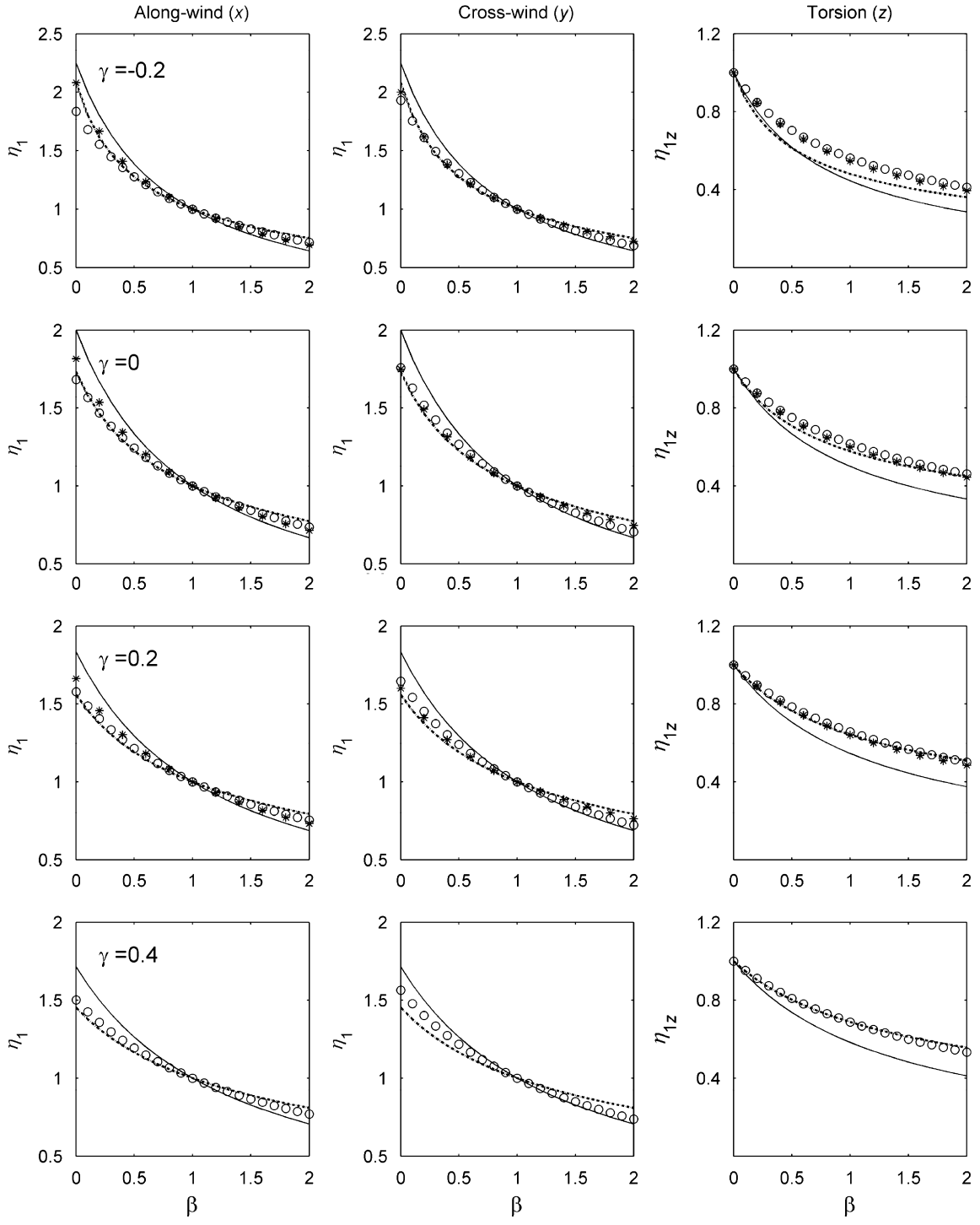

Fig. 6. Mode shape correction factors for deflections. ○: computed data from time-domain technique; *: data of circular building; solid curve: high-correlation predictions of Eqs. (3a) and (3b) and broken curve: low-correlation predictions of Eqs. (4a) and (4b).

coefficients among the wind force fluctuations on the seven levels have been calculated. The correlations for the cross-wind force fluctuations are only slightly higher than the along-wind force fluctuations. For both force directions on the circular building, the correlations are much higher than those of the along-wind

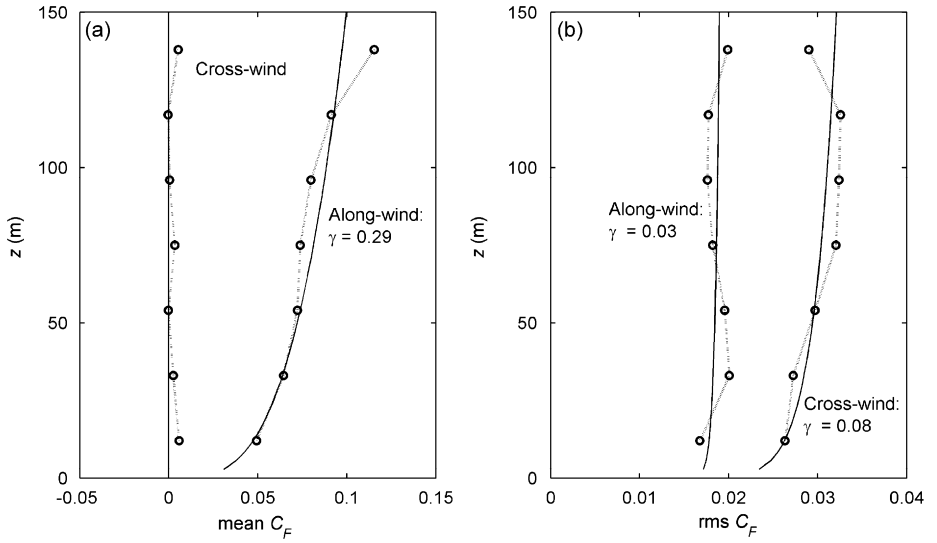

Fig. 7. Vertical distribution of force fluctuations on circular building. Symbols: wind tunnel data and line: power law fit.

excitation on the square building but slightly lower than those of the cross-wind excitation on the square building.

Assuming the same dynamic properties for the circular building as the square building, mode shape correction factors are computed for the former building for $\gamma = \{-0.2, 0, 0.2\}$. The results are plotted in Fig. 6 along with the main set of results for the square building. For the along-wind deflections, the mode shape correction factors for the circular building have values slightly yet notably more closer to the high-correlation prediction curves and more away from the low-correlation predictions when compared to the square building. This is consistent with the higher degree of correlation of along-wind wind excitation measured along the building height of the circular building. A similar observation is made for the cross-wind deflections of the circular building. It seems that the mode shape correction factor is sensitive to the degree of correlation of wind excitation along the building rather than the geometry of the building.

With the knowledge of mass distribution along the building height, mode shape correction factors for moments and torsion (and equivalent static forces) are also derived via Eq. (11). Expressions for these correction factors have been proposed by Boggs and Peterka [6] as Eq. (6). They are based on the assumption of high correlation of wind excitation. For the low-correlation case, the following expressions apply:

$$\eta_{M,\mathrm{low}} = \eta_M \times \frac{\eta_{1,\mathrm{low}}}{\eta_1} \tag{13a}$$

$$\eta_{Mz,\mathrm{low}} = \eta_{Mz} \times \frac{\eta_{1z,\mathrm{low}}}{\eta_{1z}} \tag{13b}$$

The dependence of moment correction factors, from the time-domain computation and predictions of Eqs. (6) and (13), on mode shape β is shown in Fig. 8. Results are shown for three representative values of λ: $\lambda = 0$ for uniform mass distribution; $\lambda = 1$ for building masses decreasing linearly upwards reaching zero at building top floor; and $\lambda = 0.3$ for masses decreasing to 70% of the base value at the building top. It is observed from results at other values of λ that the mode shape correction factors for moments remain almost essentially the same when λ changes between 0 and 0.3. However, when λ increases from beyond 0.3, more severe corrections are required. Fig. 8 shows the results at $\gamma = \{-0.2, 0, 2\}$ only since higher values of γ are less frequently found and the results at these values are similar to those at $\gamma = 0.2$ (Fig. 6).

For the overturning moments associated with building response along the sway directions, the correction factors are not always less than unity. At low values of λ, Figs. 8a and b, corrector factors slightly greater than unity are computed at β near 0.5. At $\lambda = 1$, Fig. 8c, the correction factors increase monotonically with β so that η_M becomes greater than unity for $\beta > 1$. Similar to the correction factors for deflection, the computed

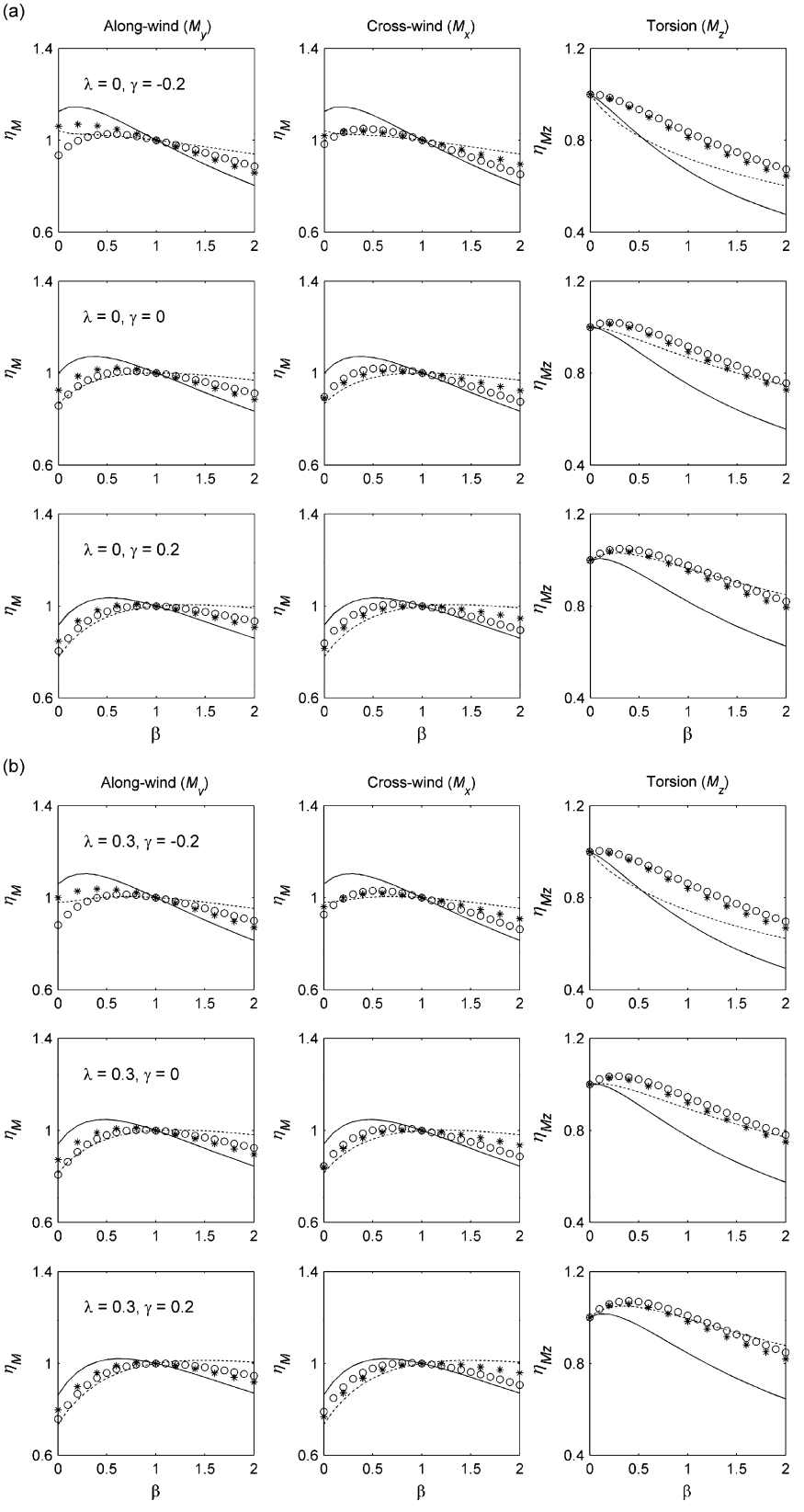
(a)
Along-wind (M_y)
Cross-wind (M_x)
Torsion (M_z)
λ = 0, γ = -0.2
λ = 0, γ = 0
λ = 0, γ = 0.2
η_M
η_{Mz}
β
(b)
Along-wind (M_y)
Cross-wind (M_x)
Torsion (M_z)
λ = 0.3, γ = -0.2
λ = 0.3, γ = 0
λ = 0.3, γ = 0.2
η_M
η_{Mz}
β

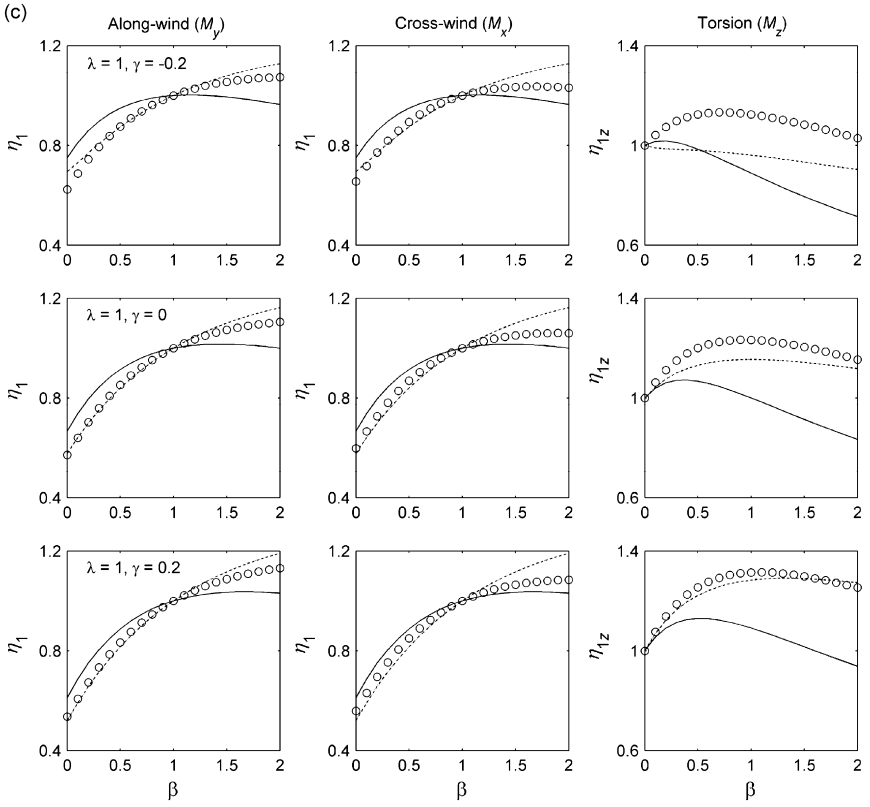

Fig. 8. (*Continued*)

data of η_M for the along-wind moment M_y fall very closely onto the low-correlation prediction curve of Eq. (13a) while the correction factors for the cross-wind moment M_x lie between the low-correlation and high-correlation curves. The results in Fig. 8 suggest that under reasonable ranges of parameters, such as $0.5 \leqslant \beta \leqslant 1.5$, $-0.2 \leqslant \gamma \leqslant 0.2$ and $\lambda \leqslant 0.3$, only mild degrees of correction are necessary with η_M between 1 ± 0.05. At $\lambda = 0$ and 0.3, results are also available for the circular building and the data are included in Figs. 8a and b. Similar to Fig. 6, the differences in the behavior of η_M from the square building can be explained by the different degrees of wind excitation correlation along the building height.

The computed data of η_{Mz} for the torsional moment are found to lie close to the low-correlation prediction curve of Eq. (13). However, when the profile of wind excitation has the negative exponent at $\gamma = -0.2$, the computed corrector factors are well above both curves of Eqs. (6b) and (13b). Another important observation is that for the common real-life mode shape at $\beta = 1$, η_{Mz} has values between 0.84 and 0.98 in Fig. 8a, values between 0.86 and 1.01 in Fig. 8b and values greater than unity in Fig. 8c. It is shown earlier in Fig. 6 that the commonly applied corrector factor at 0.7 for torsional deflections is supported by the results of η_{1z} in this study. However, it is evident now if the same correction is applied to the torsional moment assessed by the HFFB technique, the wind-induced dynamic torsion would be under-predicted.

7. Conclusions

This paper investigates the application of mode shape correction factors to the high-frequency force-balance (HFFB) technique for the assessment of wind-induced responses of a tall building. Ideal mode shapes, that is,

Fig. 8. Mode shape correction factors for moments and torsion for mass reduction factor: (a) $\lambda = 0$; (b) $\lambda = 0.3$ and (c) $\lambda = 1$. ○: computed data from time-domain technique; *: data of circular building; solid curve: high-correlation predictions of Eqs. (6a) and (6b) and broken curve: low-correlation predictions of Eqs. (13a) and (13b).

linear modes in the sway directions and constant mode in torsion, are assumed in the frequency-domain HFFB technique. Previous studies on mode shape correction factors are reviewed and it is observed that they were based on theoretical formulation of wind excitation either with perfect or no correlation along the building height. In this paper, excitation wind loads are physically measured on the wind tunnel model of a generic square tall building with a multi-channel pressure measurement system. This enables the time histories of wind forces on a number of levels along the building height to be obtained from integration of wind pressure. Wind-induced responses of the building can then be computed in the time domain with the capability of treating non-ideal mode shapes of building vibration. The computed responses are compared to the responses that would be obtained by the HFFB technique in which ideal mode shapes are assumed. Mode shape correction factors for deflections and moments are thus obtained directly.

Analysis of the measured vertical distributions of wind excitation show that they are weakly connected with the mean wind speed profile. It is also found that wind load fluctuations decreasing upwards along the building height are not uncommon. These observations are not consistent with the models used in previous studies on mode shape correction. A parametric study is thus carried out to investigate the dependence of the mode shape correction factors on the mode shapes and the vertical distributions of wind excitation and building masses. It is found that the mode shape correction factors computed directly in this study generally agree with the predictions proposed in the literature. The low-correlation predictions work better for the along-wind and torsional responses while the cross-wind responses better match the high-correlation predictions. This is in line with the degree of correlation in the wind excitations on the wind tunnel model. However, when the wind excitation decreases with height, the computed data depart significantly from the predictions in previous studies which did not apparently foresee these situations.

For the more realistic near-linear model shapes common to tall buildings with regular geometries, the HFFB technique can provide accurate predictions of the building responses only with very mild mode shape correction factors. The commonly used correction factor at 0.7 for the torsional response is found to be appropriate for the torsional deflection but not for the torsional moment.

The time-domain technique coupled with simultaneous measurement of wind pressure appeals to be a powerful tool for the computation of building responses from wind tunnel data. In addition to non-ideal modes, coupled mode shapes and higher modes can be readily treated in the method.

Acknowledgment

The investigation is a component of a group research project, HKUST 1/04C, supported by the Research Grants Council of Hong Kong.

References

[1] T. Tschanz, A.G. Davenport, The base balance technique for the determination of dynamic loads, *Journal of Wind Engineering and Industrial Aerodynamics* 13 (1983) 429–439.
[2] S. Swaddiwuhipong, M.S. Khan, Dynamic response of wind-excited building using CFD, *Journal of Sound and Vibration* 253 (2002) 735–754.
[3] A. Kareem, Model for predicting the across-wind response of buildings, *Engineering Structures* 6 (1984) 136–141.
[4] J.D. Holmes, Mode shape correction factors for dynamic response to wind, *Engineering Structures* 9 (1987) 210–212.
[5] Y.L. Xu, K.C.S. Kwok, Mode shape corrections for wind tunnel tests of tall buildings, *Engineering Structures* 15 (1993) 387–392.
[6] D.W. Boggs, J.A. Peterka, Aerodynamic model tests of tall buildings, *Journal of Engineering Mechanics* 115 (1989) 618–635.
[7] P.J. Vickery, A. Steckley, N. Isyumov, B.J. Vickery, The effect of mode shape on the wind-induced response of tall buildings, *Proceedings of the Fifth US National Conference on Wind Engineering*, Vol. 1B, Texas Tech., 1985, pp. 41–48.
[8] A. Tallin, B. Ellingwood, Analysis of torsional moments on tall buildings, *Journal of Wind Engineering and Industrial Aerodynamics* 18 (1985) 191–195.
[9] Australasian Wind Engineering Society, Wind Engineering Studies of Buildings, AWES-QAM-1-2001, 2001.
[10] H. Ueda, K. Hibi, Y. Tamura, K. Fuji, Multi-channel simultaneous fluctuating pressure measurement system and its applications, *Journal of Wind Engineering and Industrial Aerodynamics* 51 (1994) 93–104.
[11] J. Katagiri, T. Ohokuma, H. Marukawa, Analytical method for coupled across-wind and torsional wind responses with motion-induced wind forces, *Journal of Wind Engineering and Industrial Aerodynamics* 90 (2002) 1795–1805.

[12] B. Liang, Y. Tamura, S. Suganuma, Simulation of wind-induced lateral-torsional motion of tall buildings, *Computers and Structures* 26 (1997) 601–606.
[13] D.Y.N. Yip, R.G.J. Flay, A new force balance data analysis method for wind response predictions of tall buildings, *Journal of Wind Engineering and Industrial Aerodynamics* 54/55 (1995) 457–471.
[14] J.G. Zhao, K.M. Lam, Interference effects in a group of tall buildings closely arranged in an L- or T-shaped pattern, *Wind and Structures* 11 (2008) 1–18.
[15] K.M. Lam, M.Y.H. Leung, J.G. Zhao, Interference effects on wind loading of a row of closely spaced tall buildings, *Journal of Wind Engineering and Industrial Aerodynamics* 96 (2008) 562–583.
[16] A.K. Chopra, *Dynamics of Structures: Theory and Applications to Earthquake Engineering*, Prentice-Hall, Englewood Cliffs, NJ, 2000.
[17] Buildings Department, Hong Kong (BD), Code of Practice on Wind Effects in Hong Kong 2004, 2004.